High-Matching and Low-Cost Realization of the FHN Neuron Model on Reconfigurable FPGA Board

Yisu Ge , Ruyu Liu, Guodao Zhang , Mohammad Sh. Daoud , Qiwen Zhang, Xuecai Huang, Abdulilah Mohammad Mayet , Zhao-Min Chen , and Shike He

Abstract—The main objectives of neuromorphic engineering are the research, modeling, and implementation of neural functioning in the human brain. We provide a hardware solution that can replicate such a nature-inspired system by merging multiple scientific domains and is based on neural cell processes. This work provides a modified version of the original Fitz-Hugh Nagumo (FHN) neuron using a simple 2^V term called Hybrid Piece-Wised Base-2 Model (HPWBM), which accurately reproduces numerous patterns of the original neuron model. With reduced terms, we suggest modifying the original nonlinear term to achieve high matching accuracy and little computing error. Time domain and phase portraits are used to validate the proposed model, which shows that it can reproduce all of the FHN model's properties with high accuracy and little mistake. We provide an effective digital hardware approach for large-scale neuron implementations based on resource-sharing and pipelining strategies. The Hardware Description Language (HDL) is used to construct the hardware on an FPGA as a proof of concept. The recommended model hardly uses 0.48 percent of the resources on a Virtex 4 FPGA board, according to the results of the hardware implementation. The circuit can run at a maximum frequency of 448.236 MHz, according to the static timing study.

Index Terms—Neuronal models, FHN, FPGA, digital realization.

I. INTRODUCTION

SINCE neural networks, which are composed of neurons and synapses, are the basic components of the Central Nervous System (CNS), learning more about them is necessary [1], [2], [3], [4]. Numerous real-world applications of Spiking Neural Networks (SNNs) research exist, including autonomous robots, data processing, pattern recognition, and medical diagnosis. CNS is made up of a complex network of neurons, synapses, and calcium-based cells known as glia. Glia is important for safeguarding and controlling the behavior of neurons as well as synaptic connections [5], [6]. Mathematical modeling of neuronal activity is crucial for comprehending the neural network of the brain in its entirety. In order to understand and interpret the activity of biological neural networks inside the CNS, neural modeling and its processes have therefore become essential tools.

Ordinary Differential Equations (ODEs) are typically used to represent spiking neuron activities in mathematical models [7], [8], [9], [10]. To accurately reflect genuine neural actions, several models of differing degrees of complexity have been created [6], [7], [8], [9], [10], [11], [12], [13], [14], [15]. Accuracy and computing complexity of a model trade off each other, with more accurate models often needing more processing power. Hodgkin-Huxley (HH) type models [2] are appropriate if the objective is to comprehend the relationship between neuronal behavior and physiological factors, but they can be computationally demanding and may not be useful for simulations involving a high number of neurons. Spike-based models are recommended as a superior option, however, if the goal is to understand the temporal nature of spike timing and how neurons process information [12]. With only one polynomial term and no need for a reset or additional noise, the Fitz-Hugh Nagumo (FHN) neuron model [16], [17], [18] is a two-coupled differential equation model. As all nonlinear variables are basic states that can be transformed into linear and inexpensive functions for hardware implementation, it is regarded as one of the most effective dynamical models in computational neuroscience for capturing neuronal spiking characteristics.

Analog circuits and digital technologies are the two basic strategies for putting neural models into practice [10], [11],

Yisu Ge and Zhao-Min Chen are with the College of Computer Science and Artificial Intelligence, Wenzhou University, Wenzhou 325100, China (e-mail: ysg@wzu.edu.cn; chenzhaomin123@gmail.com).

Ruyu Liu is with the School of Information Science and Engineering, Hangzhou Normal University, Hangzhou 311121, China (e-mail: lry@hznu.edu.cn).

Guodao Zhang and Qiwen Zhang are with the Department of Digital Media Technology, Hangzhou Dianzi University, Hangzhou 310018, China (e-mail: guodaozhang@zjut.edu.cn; 1111812008@zjut.edu.cn).

Mohammad Sh. Daoud is with the College of Engineering, Al Ain University, Abu Dhabi 112612, UAE (e-mail: mohammad.daoud@aau.ac.ae).

Xuecai Huang and Shike He are with the Department of Neurosurgery, Lishui Municipal Central Hospital, Lishui 323000, China (e-mail: xhuang@163.com; heshikels@163.com).

Abdulilah Mohammad Mayet is with the Electrical Engineering Department, College of Engineering, King Khalid University, Abha 61411, Kingdom of Saudi Arabia (e-mail: amayet@kku.edu.sa).

Color versions of one or more figures in this article are available at https://doi.org/10.1109/TBCAS.2023.3337335.

Digital Object Identifier 10.1109/TBCAS.2023.3337335

[12], [13], [14], [15], [16], [17], [18], [19], [20], [21], [22], [23], [24], [25], [26], [27]. The final neuromorphic system is created using electrical components in the analog technique by simulating nonlinear functions in the mathematical models [21], [22], [23], [24], [25], [26], [27]. Although this method is said to be high-performance and well-developed, creating new circuits can be difficult and time-consuming. In contrast, it has been demonstrated that a digital method is a good option in terms of flexibility and extensibility [1], [2], [3], [4], [5], [6], [7], [8], [9], [10]. For real-scale neural networks to function, a high-frequency digital system is needed due to the rapid rate at which information is passed between neurons. Therefore, compared to an analog design, the digital method may be more appropriate given the high-speed needs. The digital technique is also less affected by noise and is suitable for computers and digital devices. It is also more flexible in implementation and less vulnerable to observational issues like parallax and approximation mistakes than the analog approach. In the subject of neuromorphic engineering, the use of Field Programmable Gate Arrays (FPGAs) for the digital design and implementation of neural models is very appealing, and several recent studies have been published in this area [11], [12], [13], [14], [15], [16], [17], [18], [19], [20]. After manufacture, an integrated circuit called an FPGA can be modified by the client or the designer, usually with the use of a Hardware Description Language (HDL). Large-scale digital implementations of different CNS components may be made using FPGA chips, which also offer flexibility and high speed.

The Hybrid Piece-Wised Base-2 Model (HPWBM) of FHN neuron is a modified version that is presented in this study. The polynomial term V^3 contained in the neuron model poses the biggest obstacle to its low-cost digital implementation. Using base-2 functions can be a viable and appropriate strategy depending on how these nonlinear functions behave. However, as compared to earlier efforts [6], [7], [14], and [16], the HPWBM that is being provided is significantly more accurate and does not have the identified flaws. The investigation shows that the original forms and dynamics can be successfully recreated using our modeling. Because all nonlinear components are eliminated when employing base-2 functions, there is a high matching similarity and multiplier-less implementation. This results in the creation of a digital system that is quick, inexpensive, and capable of large-scale digital realization. Since this results in a multiplier-less low-cost system using shifter-based realization, the specific novelty of our proposed model is the presentation of reduced-number power-2-based terms for nonlinear models, as well as the transformation of this high-cost and low-speed model into a very low-cost neuronal model (compared to other similar works and the original model). The large-scale digital system offered by this proposed model can recreate every part of the original FHN model with low-cost and high-speed qualities.

The paper is divided into a number of sections. In Section II, the Fitz-Hugh Nagumo model is presented. In Section III, the model's modifications and large-scale simulation testing are covered. In Section IV, the hardware is evaluated. In Section V, the paper is finally concluded.

II. FHN FORMULATION

Differential equations, which capture several facets of the neuron's response to stimuli, can be used to model and characterize the activity of neurons. The FitzHugh-Nagumo (FHN) model, a prototype of an excitable system, is one such model [16], [17], [18]. As a relaxation oscillator, this model will exhibit a distinctive excursion in phase space if the external stimulus exceeds a predetermined threshold before reverting to its resting values. This action is comparable to how spikes are produced in neurons and then gradually reduced by a slower, linear recovery variable following activation by an external current.

The following equations present this dynamical system:

$$\frac{dV}{dt} = V - W + I_{Trig} - \frac{H(V)}{3} \tag{1}$$

$$\frac{dW}{dt} = \frac{1}{T}(a - bW + V) \tag{2}$$

where

$$H(V) = V^3 \tag{3}$$

The FHN model is, in fact, a simplified form of the Hodgkin-Huxley (HH) neuron model, which simulates the activation and deactivation dynamics of a spiking neuron in great detail. The voltage variable V and the recovery variable W in the FHN formulation are used to generate distinct potential levels. The parameter I_{Trig} in this system is the stimulus current or trigger for the voltage equation. Finally, the neuron has three fixed dimensionless parameters: a, b, and T. These parameters can influence on the spiking frequency and shapes of the output signals of FHN model. As can be observed from the FHN neuron equations, some nonlinear terms (polynomial states) may result in issues with the implementation of hardware, including a decrease in hardware speed, an increase in the total system resources, and a decrease in performance and efficiency. To create a system with greater efficiency and speed while maintaining cheap costs, it is, therefore, preferable to optimize and change the underlying model.

III. MODIFICATION METHOD

In this section, we provided the proposed HPWBM, error computations, dynamic evaluations, and network behaviors.

A. HPWBM

There are a few methods for approximating calculations. The neuron models and their nonlinear components influence the choice of approximation techniques. Piece-Wised Linear (PWL), Fast Dynamic Reduction, Trigonometry, Hyperbolic, Power-2, LUT, and other techniques are examples. The total overhead costs may be lower when employing the Piece-Wised Linear (PWL) technique, but accuracy will also likely be lower and there will be some error levels. The fast-dynamic-reduced approach is used to remove one or more differential equations. Although the overhead expenses are decreased in this situation, accuracy may suffer as a result. Trigonometric approximation may be advantageous because to its high precision, but it may

TABLE I
COMPARISON BETWEEN DIFFERENT MODIFICATION METHODS FOR
NEURONAL REALIZATION

Method	Cost	Precision	Simplicity	Matching	Error
PWL	Low	Low	Simple	Low	High
Hyperbolic-Based	Middle	High	Middle	High	Middle
Trigonometric-Based	High	High	Complex	High	Middle
Fast-Dynamic-Reduced	Low	Very Low	Middle	Very Low	High
CORDIC	High	High	Complex	High	Low
LUT-Based	Low	Middle	Simple	Middle	Middle
Base-2	**Low**	**High**	**Middle**	**High**	**Low**

Fig. 1. HPWBM approximation shape based on modified method presentation. Modified method of function replacing $H(V) = V^3$ by new piece-wised base-2 term, $Z(V)$.

increase final FPGA resources and costs. The exponential terms are first converted to hyperbolic functions in the hyperbolic-based approach, but after that, the exponential terms are changed to power-2 based functions, which might increase the base-2 terms and hence increase the overall overhead costs. However, we have utilized only phrases that can be translated to shifters in power-2 based techniques. Every multiplication has been changed in this approach to a digital shifter and adder in low-cost states. This method is appropriate since it benefits from PWL and base-2 approximation, (low-cost and accurate). High levels of accuracy and matching may be attained with this method at a manageable resource cost, however our power-2-based method performs better in terms of error, matching, and precision. In our modification, we have applied the power-2 based method leads to achieving the low-cost and high-speed implementation compared to other approaches. Moreover, this method in presented in the hardware section in details. Numerous approximation strategies may be applied in this case with high precision and matching to the primary (original) model.

Specially, using the piece-wised linear method can lead to an increase in matching by increasing the number of approximation pieces, but there is an important point that with this approach, the cost of hardware implementation will also increase, and we have an implementation with high-cost attributes. This issue can also lead to a decrease in system speed. Therefore, if the number of segments of this method is low, considering the low hardware cost, the desired adaptation will also be low.

As a consequence, our goal in this paper is achieving the high-accurate digital realization of FHN neuronal model with acceptable precision and high-speed state. As can be seen in Table I, a comparison between different approximation methods is presented. The base-2 approach is selected in this case to achieve a high-accurate and low-error implementation compared with the original and other methods realization. Moreover, by removing all multiplications, the high-speed design can be achieved, significantly.

Based on (3), several approximations can be taken into account. We must assess the benefits and drawbacks of improving system performance while simultaneously lowering hardware implementation costs (total hardware resource savings) for each of these strategies. Consider the formal and uncomplicated Piece-Wised Linear (PWL) method [5]. This approach could be more affordable than others. On the other hand, the base-2 approach can be applied for modification [6], [7]. This problem may be resolved for the HPWBM of the FHN by reducing the
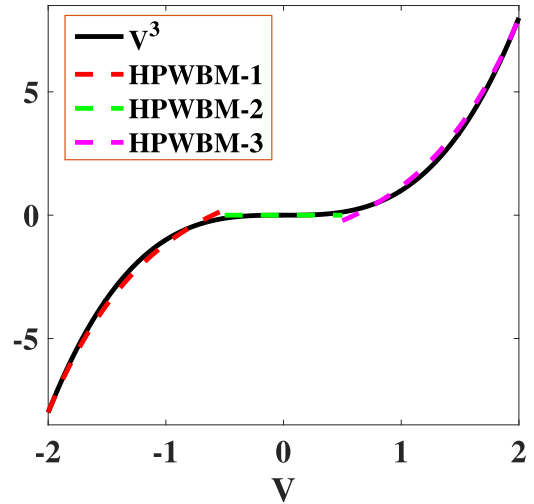
number of various base-2 functions, which results in large-scale design due to the elimination of the extra terms.

We reformulate the voltage equation of the original FHN neuron model as follows to offer a thorough grasp of the suggested approach:

$$\frac{dV}{dt} = V - W + I_{Trig} - \frac{Z(V)}{3} \quad (4)$$

where

$$Z(V) = \begin{cases} -2^{-1.66\,V} + 2; & -2 < V < -0.5 \\ 0; & -0.5 < V < 0.5 \\ 2^{1.66\,V} - 2; & 0.5 < V < 2 \end{cases} \quad (5)$$

The first stage in creating the new strategy is to create a new function to replace the major nonlinear term of the previous model, $H(V)$. Due to its symmetrical construction, as seen in Fig. 1, this function strongly resembles a base-2 wave, enabling us to approximate the polynomial nonlinear term with a base-2 function. Based on (5), we have retrieved optimized parameters using an exhaustive search technique. In the approximation process, we have used the basic fitting and curve fitting of the original nonlinear function to the new proposed function. In this approach, an exhaustive search algorithm is applied to the parameters to find their values with an improved precision. This algorithm searches for the best parameters among a set of solutions and determines the closest answer with minimum error. The scaling factors were changed to obtain a high degree of resemblance and matching between the original polynomial term and the suggested HPWBM that is shown in Fig. 2 (based on different input triggers and time constants). We succeeded in producing a new HPWBM that closely resembled the first FHN model by employing this technique. On the other hand, all multiplications in the main model may be approximated using this approximation to simple operators that are simple to implement. More information about this is provided in the hardware section. The presentation of this proposed model is
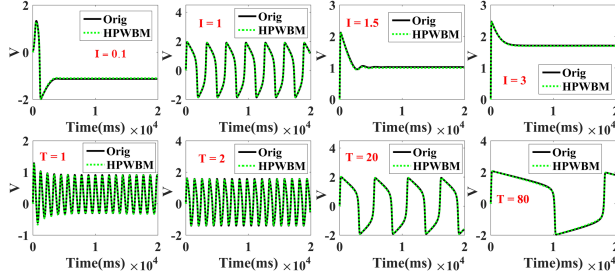
Fig. 2. HPWBM approximation shape based on modified method presentation (according to different input triggers and time constants). Modified method of function replacing $H(V) = V^3$ by new piece-wised base-2 term, $Z(V)$.

a claim that needs to be investigated and validated. In the sections that follow, we'll use several techniques to analyze and corroborate the suggested model (HPWBM). It is noticeable that selecting the parameter sets depends on evaluating all states of spiking patterns in the original and proposed models. Indeed, to have a comprehend validation process, it is essential that a range of parameter sets are considered for acceptable validation of our proposed modeling.

B. Error and Dynamic Evaluations

The HPWBM successfully and precisely reproduces the behavior of the original model, as seen in Fig. 2. To validate the proposed model, it is essential that the basic error methods are evaluated. When the proposed model is suggested, differences between the original and this proposed model must be calculated. In the neural networks, the timing process is an essential issue. Thus, in the proposed model, the spike timing must be occurred on exactly form. In this section, we examined the numerical values of the error with four primary approaches to test the correctness of the proposed model: Root Mean Square Error (RMSE) (is a frequently used measure of the differences between values (sample or population values) predicted by a model or an estimator and the values observed), Correlation (Corr) (is a criterion to evaluate statistical relationship involving dependency between two set of data), Mean Absolute Error (MAE) (is a measure of errors between paired observations expressing the same phenomenon), and Normalized Root Mean Square Error (NRMSE) [3], [4], [5], [6]. These errors are given as below:

$$\mathbf{MAE} = \frac{1}{n}\sum_{i=1}^{n}|V_{HPWBM} - V_{FHN}| \tag{6}$$

$$\mathbf{Corr} = \frac{cov(V_{FHN}, V_{HPWBM})}{\sigma_{FHN}\sigma_{HPWBM}} \tag{7}$$

$$\mathbf{RMSE} = \sqrt{\frac{\sum_{i=1}^{n}(V_{HPWBM} - V_{FHN})^2}{n}} \tag{8}$$

$$\mathbf{NRMSE} = \frac{1}{V_{max} - V_{min}}\sqrt{\frac{\sum_{i=1}^{n}(V_{HPWBM_i} - V_{FHN_i})^2}{n}} \tag{9}$$

The four errors specified for the basic variable of FHN modeling, V, is also given in Table II. Moreover, to have a quantitatively compare between our proposed model (our approximation

TABLE II
ERROR VALUES COMPARISON BETWEEN OUR HPWBM AND OTHER SIMILAR WORKS [16], [17], [18], [19]

Variables	MAE	RMSE	Corr%	NRMSE %	MRE %
V in HPWBM	0.0034	0.019	99.8	0.4	1.02
V in [16]	-	-	-	-	-
V in [17]	0.03	0.45	84	1.15	1.27
V in [18]	0.04	0.32	-	3.42	-
V in [19]	0.015	0.057	-	1.43	1.52

TABLE III
THE TYPE OF EQUILIBRIUM POINTS AND THEIR COORDINATES

Variables	Original	HPWBM
V and W I_{Trig}=0.5	Nodal sink(-0.78,-0.15)	Nodal sink(-0.75,-0.12)
V and W I_{Trig}=1	Nodal sink(0.53,1.18)	Nodal sink(0.49,1.22)

All nodal sink point are stable.

method which leads to voltage signal accuracy by the original model) and other similar models [16], [17], [18], [19], a comparison is presented based on the error levels. It is clear from Table II's error values that the suggested model delivers the findings with excellent precision (leads to use base-2 approximation approach).

In case of dynamic consideration, when modeling the change from the rest and spike states, the communication between the two nullcline equations is particularly important [10], [11], [12], [13], [14]. Equilibrium points appear where the equation nullclines cross. For dynamic assessment, we consider a dynamic system with two variables. Here, V and W are assessed using a variable V, and the voltage signal (V) is regarded as a basic and common variable. The equations of the original model contain many nullclines:

$$\frac{dV}{dt} = 0 \implies V = W - I_{Trig} + \frac{V^3}{3} = 0 \tag{10}$$

$$\frac{dW}{dt} = 0 \implies W = \frac{V + a}{b} = 0 \tag{11}$$

By inputting the fixed values from Table III, the following points are generated to describe and explain the coupling of the two variables V and W.

$$\begin{cases} S = \frac{dV}{dt} = V - W + I_{Trig} - \frac{H(V)}{3} \\ N = \frac{dW}{dt} = \frac{1}{T}(a - bW + V) \end{cases} \tag{12}$$

The bifurcation analysis of equilibrium points requires a Jacobian matrix and eigenvalues:

$$J(V, W) = \begin{bmatrix} L & O \\ P & Y \end{bmatrix} \tag{13}$$

where

$$\begin{cases} L = \frac{\partial S}{\partial V} , & O = \frac{\partial S}{\partial W} \\ P = \frac{\partial N}{\partial V} , & Y = \frac{\partial N}{\partial W} \end{cases} \tag{14}$$

Considering the stability of equilibrium points, the sign of $(L + Y)$ must be analyzed. If $(L + Y) < 0$, the system is stable and otherwise, it is unstable.
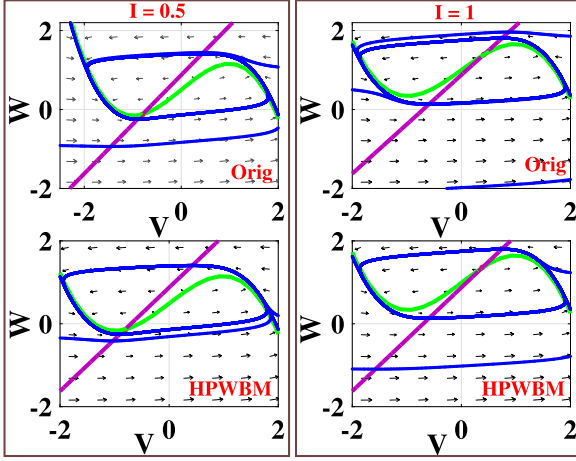
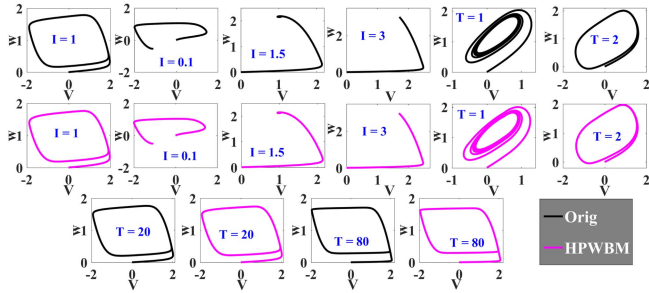Fig. 3. Equilibrium points presentation of original and HPWBM based on two different I_{Trig}.

Fig. 4. Different patterns of phase portraits for the original and proposed models (according to different input triggers and time constants).

Fig. 5. 1000 neurons' activity for the original FHN and proposed HPWBM models in a raster plot.

For suggested model (HPWBM), Jacobian matrixe for variable V and W is computed (similar to original model process). Table III includes the coordinates and types of equilibrium. Bifurcation theory and changes in model parameters can be used to classify various modes. The stability or instability of equilibrium points is dictated by the main diameter of the Jacobin matrix's parameters. When the total of the parameters in the Jacobian matrix's initial diameter is less than zero (negative), an equilibrium point is said to be stable. If it is higher than zero, it is said to be unstable (positive). The original and proposed models dynamics are depicted in Fig. 3. As can be seen, the HPWBM follows the FHN model, accurately. Also provided and contrasted in Fig. 4 are the phase portraits of the original and suggested models (based on various linked variables). As can be seen, the proposed model can follow the original one in high-degree of matching.

C. Network Behavior

A network of 1000 randomly linked neurons is simulated to implement the modified model at the network size. Taking inspiration from the structure of a mammalian cortex, we opted for a ratio of 4 to 1 between excitatory and inhibitory neurons, and strengthened the inhibitory synaptic connections. In Fig. 5, the simulations' raster plots are displayed. The modified model and t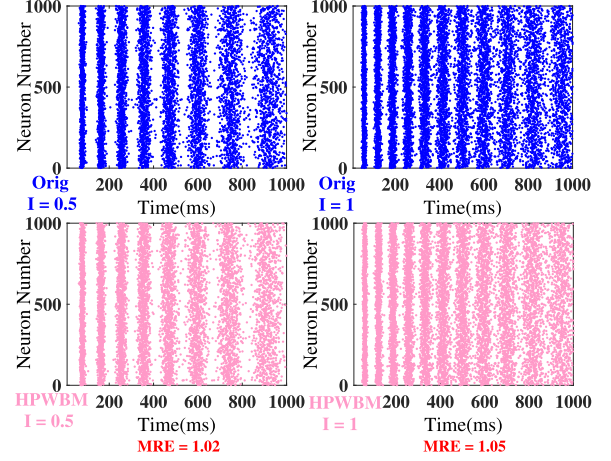he original model in network behaviors have a lot of structural similarities. Mean Relative Error (MRE) is computed to compare the original and modified network behavior models. Fig. 5 also displays this error parameter's value. According to Fig. 5 and the error values, another indication of the suggested model's correctness is the network scale, where it is clear that the behavior of the original and proposed models behave similarly to one another.

IV. HARDWARE REALIZATION

The digital implementation of HPWBM is shown in this section. The bit width for a digital implementation must first be chosen. The bit width must be selected in a way that prevents overflow with left and right shifts, which is an essential consideration. The overall architecture for the final system produced in the second stage, which discretizes the differential equations using the Euler technique. The third phase involves the Hardware Description Language (HDL) evaluating this architecture before they can be implemented on the Virtex-4 FPGA device. Here are the specifics of these actions.

A. Equations Discretization

There are different methods for implementing approximate equations in discretization domain. In the meantime, one of the simplest and least expensive possible methods is to use Euler's method, which is very straightforward and simply performs the discretization operation. In fact, because our goal is to implement hardware with the lowest cost, we have chosen Euler's method. To be suitable for the FPGA board, discretized equations make up the suggested model. The Euler technique is used for this discretization. The Euler approach calls for a solution to:

$$\frac{dK}{dt} = E(t) \qquad (15)$$

we have

$$\frac{K[i+1] - K[i]}{dt} = E(t) \longrightarrow K[i+1] = K[i] + dtE(t) \qquad (16)$$
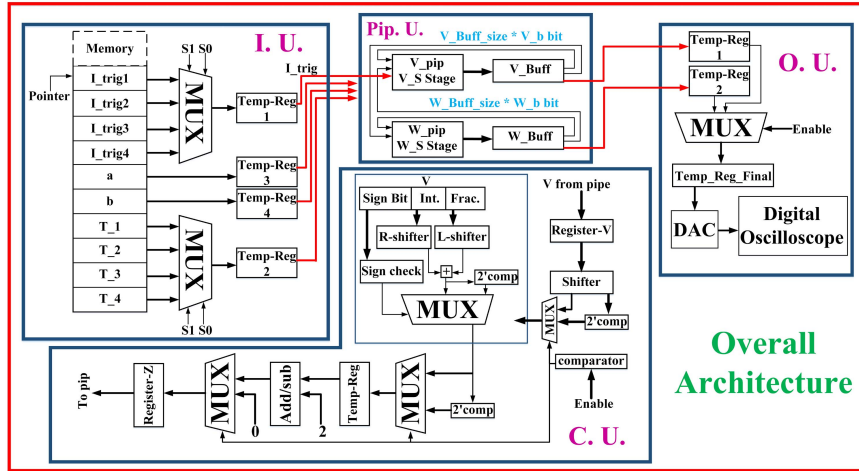
Where K and E are two typical variables.

Fig. 6. Overall architecture of the proposed HPWBM.

The time step, dt, which serves as a multiplier in (12), has a value of $\frac{1}{128}$, or 7 right shifts. This eliminates the parameter's multiplication action. In a manner similar to this, it is also feasible to acquire a multiplier-less implementation, which is specifically covered in the parts that follow. It should be noted that the original and suggested models' time steps in all simulations are $\frac{1}{128}$. There have been tests using various time steps. This amount acts as a suitable time step for a good match between the models. Selecting a lower time step makes the system more complicated, but the accuracy does not alter in a meaningful way.

B. Overall Architecture

Fig. 6 shows the overall architecture for HPWBM. As can be seen in this architecture, the first unit, Input Unit (I. U.) is responsible for generating required data for triggering the neurons. On the other hand, the Pipelining Unit (Pip. U.) provides the final signals of the proposed voltages (in the HPWBM). The pipeline strategy will be used in this section to enhance the frequency of the neurons. Two buffers (V_{Buff} and W_{Buff}) are taken into consideration for a pipeline implementation of the suggested HPWBM. In this diagram, V_S and W_S stages, respectively, are used to actualize $V_{p}ip$ and $W_{p}ip$. V_{Buff} and W_{Buff} are the storage blocks in this illustration. The bit-width of each unit in the buffers is the same as that in the $V_{p}ip$ and $W_{p}ip$ modules, which are chosen based on the precision needed. As a result, the following prerequisites must be met:

$$\begin{cases} N = V_{Buf-Size} + V_{Stage} = W_{Buf-Size} + W_{Stage} \\ V_{Buf-Size} = W_{Buf-Size} \\ V_{Stage} = W_{Stage} \end{cases} \quad (17)$$

Synchronization between the W and V structures is required for the pipeline structure to operate properly (and meet the third equation). Moreover, the Output Unit (O. U.) is responsible for generating the final target signals (for two basic variables of HPWBM). Finally, the important parts of this architecture is Control Unit (C. U.) which provides the required signals for controlling the pipelining unit and also, generating the necessary signals that help to produce the basic voltage variable in the HPWBM. In this submodule, the basic proposed term of the HPWBM ($Z(V)$), is calculated using the base-2 module calculator.

C. Bit-Width Specification

In general, numbers are displayed in digital in both fixed-point and floating-point forms. Floating-point display shows numbers with much more precision than fixed-point, but at the same time, in terms of implementation, it consumes more digital resources and cause speed-down in the final circuit. In practice and in most processing systems that are implemented with FPGA, especially when speed is important and resources are limited, the fixed-point method is used. Fixed-point representation is applied for depicting the variables and parameters in digital implementation. Thus, the range of all variables in digital design is computed. With 5 bits for the integer, 15 bits for the fraction, and 1 b for the sign, our proposed model has a final bit-width of 21 bits. This is based on the maximum and lowest constant values, the number of bits (in terms of the maximum left and right shift), overall architecture, and the necessity to prevent any overflow. For more explanations, in case of bit-width determination, we have applied the fixed-point way. In this approach, at first, it should be determined all maximum and minimum values of signals and variables in the proposed model and second, the maximum shift must be calculated for avoiding any overflows in data. In our proposed model, the variable V range is between -2 to 2. Also, the variable W range is between -0.5 to 1.5. The other parameters are as: (a=0.8, b=0.7, T=13). Also, the maximum number of T=80 (which write as $\frac{1}{T}$ that means shifts to right in fraction part). The maximum number of $I_{Trig} = 3$. Thus, based on the maximum integer value of our proposed model ($I_{Trig} = 3$), we have selected 5 bits for integer with sign bit. On the other hand, based on digital realization of model, the maximum right shift also must be calculated (due to eliminating all multiplications). By this calculation, the bit-width of 15 is considered for fraction part (due to converting time step dt to
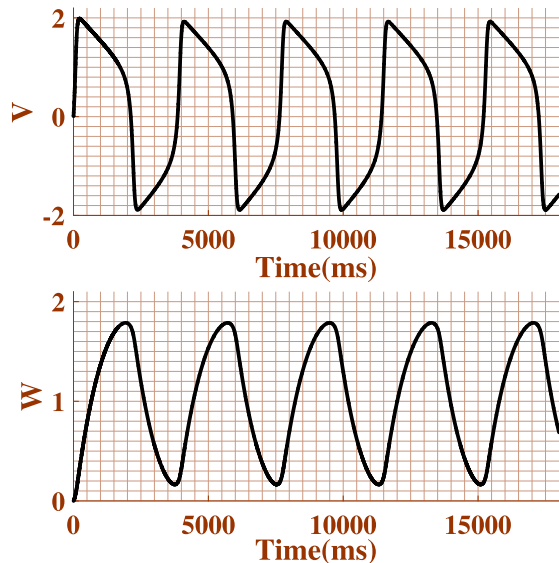
Fig. 7. Digital oscilloscope output of the proposed HPWBM on Virtex-4 FPGA.

TABLE IV
COMPARISON BETWEEN PROPOSED APPROACH AND PREVIOUSLY PUBLISHED PAPERS

Ref.	Slices %	FFs %	LUTs %	Freq. (MHz)
Orig. (Virtex 4)	2	1	1	119
HPWBM (Virtex 4)	0.48	0.27	0.32	377
[16] (Virtex 2)	46	18	38	0
[17] (Virtex 2)	2.68	1.66	3.32	175
[18] (Virtex 2)	3	2	1	0
[19] (Virtex 4)	1	1	1	320

TABLE V
H-SE FOR VALIDATING THE IMPLEMENTATION ACCURACY

Applied Stimulus	$\mathbf{H} - \mathbf{SE}$
$I = 0.1$	0.0061
$I = 1$	0.0044
$I = 1.5$	0.0065

digital shift to right). Indeed, the term $\frac{1}{dt*T}$ requires 15 b right shift for validation. Finally, 21-bit is considered for all parts of the digital system as fixed-point case. Consequently, all parts of our digital system uses the fixed-point case.

All the components of the Fig. 6 have been realized based on the fixed bit width of 21. According to Fig. 6, each part that finishes its calculations produces an output corresponding to the width of 21 bits and sends it to the next part. Similarly, the rest of the sections work with 21 b width. So since our bit width is fixed, the effects of changing it have no effect on it. In fact, we have a fixed bit width that is fixed in all digital systems. Therefore, we do not need to adjust the bit width of signals and parameters of the desired shape. All parts of this architecture work with a fixed bit width of 21 bits.

D. Realization Results

Results of the hardware-digital HPWBM implementation are shown in this section. The suggested model was developed on the FPGA platform Virtex-4. The output of the digital oscilloscope demonstrates that the approximation model accurately and closely reproduces the behavior of the original model. The model was created using Verilog in the Xilinx ISE program. The V and W signals' digital oscilloscope output is shown in Fig. 7. This figure demonstrates how closely the digital oscilloscope's output resembles the behavior of the original device. An 8-bit DAC is applied for converting the digital data to analog one for representing them on the digital oscilloscope. The original model, as previously stated and according to (1), (2), and (3), employs a significant number of multiplication, division, and nonlinear functions. Due to the FPGA's powerful processing capabilities, the equations from the original model may be implemented directly on the device without any approximation. Yet, this results in a decrease in processing frequency and a rise in the utilization of hardware resources, making hardware

implementation ineffective and subpar. All of the previous model's nonlinear parts and functions, which are expensive to implement on hardware, have been swapped out with functions in the proposed model that are substantially less expensive to implement on hardware. These high-precision alternative functions, which are well described, provide a superior hardware implementation than the original model. They also result in a decrease in the number of hardware resources used and an increase in FPGA operating frequency. Table IV shows the hardware resources and frequency for the primary and suggested models of FHN and other similar papers which implemented on the Virtex-4 and Virtex-2 reconfigurable boards (FPGA).

The comparison of resource use presented in Table IV amply demonstrates the suggested model's savings in the utilization of hardware resources. Additionally, the HPWBM operating frequency implies that the suggested model performs almost 3.77 times more quickly than the original model. The system's overall performance is enhanced in our recommended model by substituting expensive modules like multipliers, divisions, and polynomial terms, with approximation functions that have a significantly lower cost, as evidenced by the aforementioned justifications and Table IV. Additionally, by applying the pipeline technique to HPWBM, the final overhead costs of FPGA are reduced, significantly compared to other similar papers. Also, the maximum frequency of our proposed model is higher than the other works. The attributes of low-cost approach help to achieve a large-scale digital system due to reducing the FPGA resources costs compared to other FHN works in this field. It is mentioned that, in Table IV, some frequencies are fixed to 0 value due to no frequency reports in the cited papers.

Moreover, for considering the accuracy of the digital implementation, the other table (Table V), is presented. As can be seen in this table, for three cases of stimulus currents, the Hardware-Simulation Error (H-SE) is calculated to validate the accuracy of realization. This H-SE is computed based on the following formulation:

$$\mathbf{H} - \mathbf{SE} = |V_{Simulation} - V_{Hardware}| \qquad (18)$$

The high-accuracy digital realization of the FHN neural model with acceptable precision and high-speed state is what we are

aiming for in this study. Additionally, it is possible to dramatically increase design speed by doing away with all multiplications. The other efforts in this subject that may be assessed, notably, in terms of FPGA implementation are described in this strategy for neuromorphic realization and implementation [28], [29], [30], [31], [32], [33], [34], [35], [36], [37], [38], [39].

V. CONCLUSION

In this article, the HPWBM is digitally implemented. By deleting the original FHN model's nonlinear functions, which are difficult to digital realization, we were able to create the approximated model. By doing this, we were able to achieve two characteristics of the ideal implementation: low hardware cost and high frequency. In addition to the proposed model's acceptable accuracy, it is evident from a comparison of the synthesis results between it and the primary model on the FPGA board that the proposed model is superior to the original model in terms of its efficient use of hardware resources, operating frequency, and energy consumption. In conclusion, it can be concluded from the data that the suggested model consumes fewer hardware resources, and roughly 3.77 times as much frequency as the original model. Lastly, to handle increasingly complicated models with more biological components, the suggested model may be further enhanced in terms of hardware capacity and speed as part of future studies. As a result, this work (HPWBM) that has been described represents a more efficient approach towards the digital implementation of FHN compared to the previous works. The given results can be used as inspiration to work with more intricate models that produce great accuracy in biological neurons. To create artificial organs, fully assess biological cell activity and associated disorders, cure diseases, run laboratory simulations, etc., it is necessary to improve outcomes and use more biological models.

REFERENCES

[1] M. A. Imani, A. Ahmadi, M. RadMalekshahi, and S. Haghiri, "Digital multiplierless realization of coupled Wilson neuron model," *IEEE Biomed. Circuits Syst.*, vol. 12, no. 6, pp. 1431–1439, Dec. 2018.

[2] T. Luo et al., "An FPGA-Based hardware emulator for neuromorphic chip with RRAM," *IEEE Trans. Comput.-Aided Des. Integr. Circuits Syst.*, vol. 39, no. 2, pp. 438–450, Feb. 2020.

[3] S. Haghiri, A. Ahmadi, and M. Saif, "VLSI implementable neuron-astrocyte control mechanism," *Neurocomputing*, vol. 214, pp. 280–296, Nov. 2016.

[4] S. Haghiri, A. Ahmadi, and M. Saif, "Complete neuron-astrocyte interaction model: Digital multiplierless design and networking mechanism," *IEEE Trans. Biomed. Circuits Syst.*, vol. 11, no. 1, pp. 117–127, Feb. 2017.

[5] M. Ghanbarpour, A. Naderi, S. Haghiri, and A. Ahmadi, "An efficient digital realization of retinal light adaptation in cone photoreceptors," *IEEE Trans. Circuits Syst.-I: Regular Papers*, vol. 68, no. 12, pp. 5072–5080, Dec. 2021.

[6] S. Haghiri and A. Ahmadi, "A novel digital realization of AdEx neuron model," *IEEE Trans. Circuits Syst.-II: Exp. Briefs*, vol. 67, no. 8, pp. 1444–1448, Aug. 2020.

[7] M. Ghanbarpour, A. Naderi, S. Haghiri, B. Ghanbari, and A. Ahmadi, "Efficient digital realization of endocrine pancreatic β-cells," *IEEE Trans. Biomed. Circuits Syst.*, vol. 17, no. 2, pp. 246–256, Apr. 2023, doi: 10.1109/TBCAS.2023.3233985.

[8] M. Heidarpour, A. Ahmadi, and R. Rashidzadeh, "A CORDIC based digital hardware for adaptive exponential integrate and fire neuron," *IEEE Trans. Circuits Syst.-I: Regular Papers*, vol. 63, no. 11, pp. 1986–1996, Nov. 2016.

[9] H. Soleimani, M. Bavandpour, A. Ahmadi, and D. Abbott, "Digital implementation of a biological astrocyte model and its application," *IEEE Trans. Neural Netw.*, vol. 26, no. 1, pp. 127–139, Jan. 2015.

[10] H. Soleimani and E. M. Drakakis, "An efficient and reconfigurable synchronous neuron model," *IEEE Trans. Circuits Syst. II: Exp. Briefs*, vol. 65, no. 1, pp. 91–95, Jan. 2018, doi: 10.1109/TCSII.2017.2697826.um.

[11] M. Heidarpur, A. Ahmadi, M. Ahmadi, and M. R. Azghadi, "CORDIC-SNN: On-FPGA STDP learning with izhikevich neurons," *IEEE Trans. Circuits Syst.-I: Regular Papers*, vol. 66, no. 7, pp. 2651–2661, Jul. 2019, doi: 10.1109/TCSI.2019.2899356.

[12] H. Soleimani, A. Ahmadi, and M. Bavandpour, "Biologically inspired spiking neurons: Piecewise linear models and digital implementation," *IEEE Trans. Circuits Syst. I., Regular Papers*, vol. 59, no. 12, pp. 2991–3004, Dec. 2012.

[13] K. Akbarzadeh-Sherbaf, B. Abdoli, S. Safari, and A.-H. Vahabie, "A scalable FPGA architecture for randomly connected networks of Hodgkin-Huxley neurons," *Front. Neurosci.*, vol. 68, no. 12, Dec. 2021, Art. no. 698.

[14] S. Haghiri, A. Naderi, B. Ghanbari, and A. Ahmadi, "High speed and low digital resources implementation of Hodgkin-Huxley neuronal model using Base-2 functions," *IEEE Trans. Circuits Syst. I: Regular Papers*, vol. 68, no. 1, pp. 275–287, Jan. 2021.

[15] J. Chung, T. Shin, and J. S. Yang, "Simplifying deep neural networks for FPGA-Like neuromorphic systems," *IEEE Trans. Comput.-Aided Des. Integr. Circuits Syst.*, vol. 38, no. 11, pp. 2032–2042, Nov. 2019.

[16] M. Nouri, G. H. R. Karimi, A. Ahmadi, and D. Abbott, "Digital multiplierless implementation of the biological FitzHugh—Nagumo model," *Neurocomputing*, vol. 165, pp. 468–476, 2015.

[17] A. Zahedi, S. Haghiri, and M. Hayati, "Multiplierless digital implementation of time-varying FitzHugh—Nagumo model," *IEEE Trans. Circuits Syst. I: Regular Papers*, vol. 66, no. 7, pp. 2662–2670, Jul. 2019.

[18] M. Hayati, M. Nouri, S. Haghiri, and D. Abbott, "A digital realization of astrocyte and neural glial interactions," *IEEE Trans. Biomed. Circuits Syst.*, vol. 10, no. 2, pp. 518–529, Apr. 2016.

[19] S. Haghiri, S. I. Yahya, A. Rezaei, and A. Ahmadi, "Multiplierless implementation of Fitz-Hugh Nagumo (FHN) modeling using CORDIC approach," *IEEE Trans. Emerg. Topics Comput. Intell.*, early access, Aug. 3, 2023, doi: 10.1109/TETCI.2023.3300176.

[20] H. Soleimani, A. Ahmadi, M. Bavandpour, and O. Sharifipoor, "A generalized analog implementation of piecewise linear neuron models using CCII building blocks," *Neural Netw.*, vol. 51, pp. 26–38, 2014.

[21] O. Sharifipoor and A. Ahmadi, "An analog implementation of biologically plausible neurons using CCII building blocks," *Neural Netw.*, vol. 36, pp. 129–135, 2012.

[22] S. Millner, A. Grübl, K. Meier, J. Schemmel, and M. O. Schwartz, "A VLSI implementation of the adaptive exponential integrate-and-fire neuron model," in *Proc. Annu. Conf. Neural Inf. Process. Syst.*, 2010, pp. 1642–1650.

[23] S. Brink et al., "A learning-enabled neuron array IC based upon transistor channel models of biological phenomena," *IEEE Trans. Biomed. Circuits Syst.*, vol. 7, no. 1, pp. 71–81, Feb. 2013.

[24] Y. Yamashita and H. Torikai, "A novel PWC spiking neuron model: Neuron-like bifurcation scenarios and responses," *IEEE Trans. Circuits Syst. I: Regular Papers*, vol. 59, no. 11, pp. 2678–2691, Nov. 2012.

[25] J. A. Starzyk and Basawaraj, "Memristor crossbar architecture for synchronous neural networks," *IEEE Trans. Circuits Syst. I: Regular Papers*, vol. 61, no. 8, pp. 2390–2401, Aug. 2014.

[26] Y. Wang and S.-C. Liu, "A two-dimensional configurable active silicon dendritic neuron array," *IEEE Trans. Circuits Syst. I., Regular Papers*, vol. 58, no. 9, pp. 2159–2171, Sep. 2011.

[27] G. Indiveri et al., "Neuromorphic silicon neuron circuits," *Front. Neurosci.*, vol. 5, no. 73, pp. 1–23, 2011.

[28] J. E. Volder, "The cordic trigonometric computing technique," *IRE Trans. Electron. Comput.*, vol. EC-8, no. 3, pp. 330–334, Sep. 1959.

[29] J. Walther, "The story of unified cordic," *J. VLSI Signal Process. Syst. Signal, Image, Video Technol.*, vol. 25, no. 2, pp. 107–112, 2000.

[30] S. Song, K. D. Miller, and L. F. Abbott, "Competitive Hebbian learning through spike-timing-dependent synaptic plasticity," *Nature Neurosci.*, vol. 3, no. 9, pp. 919–926, 2000.

[31] J.-P. Pfister and W. Gerstner, "Triplets of spikes in a model of spike timing-dependent plasticity," *J. Neurosci.*, vol. 26, no. 38, pp. 9673–9682, Sep. 2006.

[32] G. Indiveri1 et al., "Neuromorphic silicon neuron circuits," *Front. Neurosci.*, vol. 5, 2011, Art. no. 9202, doi: 10.3389/fnins.2011.00073.

[33] E. Jokar, H. Abolfathi, A. Ahmadi, and M. Ahmadi, "An efficient uniform-segmented neuron model for large-scale neuromorphic circuit design: Simulation and FPGA synthesis results," *IEEE Trans. Circuits Syst. I: Regular Papers*, vol. 66, no. 6, pp. 2336–2349, Jun. 2019, doi: 10.1109/TCSI.2018.2889974.

[34] M. Ghanbarpour, A. Naderi, B. Ghanbari, S. Haghiri, and A. Ahmadi, "Digital hardware implementation of Morris-Lecar, Izhikevich, and Hodgkin-Huxley neuron models with high accuracy and low resources," *IEEE Trans. Circuits Syst. I: Regular Papers*, vol. 70, no. 11, pp. 4447–4455, Nov. 2023, doi: 10.1109/TCSI.2023.3303941.

[35] N. Qiao et al., "A reconfigurable on-line learning spiking neuromorphic processor comprising 256 neurons and 128K synapses," *Front. Neurosci.*, vol. 9, 2015, Art. no. 141, doi: 10.3389/fnins.2015.00141.

[36] C. Frenkel, M. Lefebvre, J. Legat, and D. Bol, "A 0.086-mm^2 12.7-pJ/SOP 64k-Synapse 256-Neuron online-learning digital spiking neuromorphic processor in 28nm CMOS," *IEEE Trans. Biomed. Circuits Syst.*, vol. 13, no. 1, pp. 145–158, Feb. 2019.

[37] E. Jokar, H. Soleimani, and E. M. Drakakis, "Systematic computation of nonlinear bilateral dynamical systems with a novel low-power log-domain circuit," *IEEE Trans. Circuits Syst. I: Regular Papers*, vol. 64, no. 8, pp. 2013–2025, Aug. 2017.

[38] C. Frenkel, J. Legat, and D. Bol, "MorphIC: A 65-nm 738k-Synapse/mm^2 quad-core binary-weight digital neuromorphic processor with stochastic spike-driven online learning," *IEEE Trans. Biomed. Circuits Syst.*, vol. 13, no. 5, pp. 999–1010, Oct. 2019, doi: 10.1109/ISCAS.2019.8702793.

[39] E. Jokar and H. Soleimani, "Digital multiplierless realization of a calcium-based plasticity model," *IEEE Trans. Circuits Syst. II: Exp. Briefs*, vol. 64, no. 7, pp. 832–836, Jul. 2017.

Yisu Ge is with Wenzhou University, Wenzhou, China. His research interests include visual object tracking, object detection and neural network compression.

Ruyu Liu received the Ph.D. degree in control science and engineering from the Zhejiang University of Technology, Hangzhou, China, in 2021. She is currently with the School of Information Science and Technology, Hangzhou Normal University, Hangzhou. Her research interests include 3D vision and deep learning.

Guodao Zhang received the Ph.D. degree from the Zhejiang University of Technology, Hangzhou, China, in 2022. His main research interests include computational intelligence, Internet of Things, process mining, virtual reality.

Mohammad Sh. Daoud received the Ph.D. degree in computer science from De Montfort University, Leicester, U.K. He is currently an Associate Professor with the College of Engineering, Al Ain University, Al Ain, United Arab Emirates. His research interests include artificial intelligence, swarm systems, secured systems and networks, and smart applications.

Qiwen Zhang received the bachelor's degree from Guizhou Normal University, Guiyang, China, in 2023. Her main research interests include machine learning and data mining.
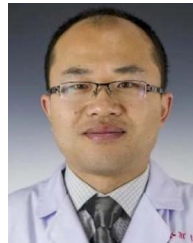
Xuecai Huang received the graduation degree from Kunming Medical University, Kunming, China, in 2006. He has accumulated rich clinical experience in the diagnosis and treatment of severe craniocerebral injury, cerebrovascular diseases and intracranial tumors, and has in-depth research in the diagnosis and treatment of severe cerebral aneurysm rupture and hemorrhage, and is good at microneurosurgical operations such as brain tumors, cerebrovascular diseases, facial muscle tics and trigeminal neuralgia microvascular decompression.

Abdulilah Mohammad Mayet received the M.Sc. and Ph.D. degrees from the King Abdullah University of Science and Technology, Thuwal, Saudi Arabia. He is currently a 2030 Leader with MiSK Foundation. He has research collaboration with the University of California Irvine, Irvine, CA, USA, and Cornell University, Ithaca, NY, USA. He is currently an Assistant Professor with King Khalid University, Abha, Saudi Arabia, teaching courses in Nanofabrication and FPGA for AI. He is also the Director of the Engineering College Research Center and Consultant with Artificial Intelligence Center.

Zhao-Min Chen received the B.S. degree from Hunan University, Changsha, China, in 2016, and the Ph.D. degrees from the Department of Computer Science and Technology, Nanjing University, Nanjing, China, in 2021. He is currently an Associate Professor with Wenzhou University, Wenzhou, China. He has authored or coauthored several academic papers on international journals and international conferences, including IEEE TRANSACTIONS ON PATTERN ANALYSIS AND MACHINE INTELLIGENCE, IEEE TRANSACTIONS ON IMAGE PROCESSING, IEEE TRANSACTIONS ON IMAGE PROCESSING, PR, CVPR, ECCV and among others. His research interests include deep learning, computer vision, general object detection and multi-label image recognition.
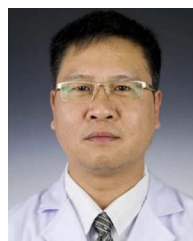
Shike He received the graduation from the Zhejiang University School of Medicine, Hangzhou, China, in 1993, majoring in clinical medicine. Taking the lead in carrying out the interventional diagnosis and treatment technology of cerebrovascular diseases in our city, we have completed the interventional diagnosis and treatment of more than 200 cases of cerebrovascular diseases every year, and are good at the interventional surgery of patients with intracranial aneurysm, cerebral arteriovenous malformation, dural arteriovenous fistula and intracranial artery injury, as well as the treatment of patients with brain tumors, severe craniocerebral injury and cerebral hemorrhage.